

# Deployable Reinforcement Learning with Variable Control Rate

Dong Wang<sup>1</sup>, Giovanni Beltrame<sup>2</sup>

<sup>1</sup> dong-1.wang@polymtl.ca

<sup>2</sup> giovanni.beltrame@polymtl.ca

## Abstract

Deploying controllers trained with Reinforcement Learning (RL) on real robots can be challenging: RL relies on agents' policies being modeled as Markov Decision Processes (MDPs), which assume an inherently discrete passage of time. The use of MDPs results in that nearly all RL-based control systems employ a fixed-rate control strategy with a period (or time step) typically chosen based on the developer's experience or specific characteristics of the application environment. Unfortunately, the system should be controlled at the highest, worst-case frequency to ensure stability, which can demand significant computational and energy resources and hinder the deployability of the controller on onboard hardware. Adhering to the principles of reactive programming, we surmise that applying control actions *only when necessary* enables the use of simpler hardware and helps reduce energy consumption. We challenge the fixed frequency assumption by proposing a variant of RL with *variable control rate*. In this approach, the policy decides the action the agent should take as well as the duration of the time step associated with that action. In our new setting, we expand Soft Actor-Critic (SAC) to compute the optimal policy with a variable control rate, introducing the Soft Elastic Actor-Critic (SEAC) algorithm. We show the efficacy of SEAC through a proof-of-concept simulation driving an agent with Newtonian kinematics. Our experiments show higher average returns, shorter task completion times, and reduced computational resources when compared to fixed rate policies.

## Introduction

Temporal aspects of reinforcement learning (RL), such as the duration of the execution of each action or the time needed for observations, are frequently overlooked. This oversight arises from the foundational hypothesis of the Markov Decision Process (MDP), which assumes the independence of each action undertaken by the agent (Norris 1998). As depicted in the top section of Figure 1, conventional RL primarily focuses on training an action policy, generally neglecting the intricacies of policy implementation. Some prior research approached the problem by splitting their control algorithm into two distinct components (Williams et al. 2017): a learning part responsible for proposing an action policy, and a control part responsible for

implementing the policy (Yang et al. 2018; Zanon and Gros 2020; Mahmood et al. 2018).<sup>1</sup>

Translating action policies composed of discrete time steps into real-world applications generally means using a fixed control rate (e.g., 10 Hz). Practitioners typically choose the control rate based on their experience and the specific needs of each application, often without considering adaptability or responsiveness to changing environmental conditions. Imagine driving a car in a straight line in an extensive environment without obstacles: very few control actions are needed. On the contrary, driving in tight spaces with low tolerances and following complex paths can require a higher control frequency. Setting the control frequency is set to a fixed value requires it to be the worst-case (or an average if safety is not a concern) scenario that allows controllability of the system. In practical applications of reinforcement learning, especially in scenarios with constrained onboard computer resources, maintaining a consistently high fixed control rate can limit the availability of computing resources for other tasks and significantly increase energy consumption.

Furthermore, the inherent inertia of physical systems cannot be ignored, impacting the range of feasible actions. In such cases, an agent's control actions are closely tied to factors like velocity and mass, leading to considerably different outcomes when agents execute the same actions at different control rates.

Hence, applying RL directly to real-world scenarios can be challenging when the temporal dimension is not considered. The typical approach is to employ *a fast enough but fixed control rate that accommodates the worst-case scenario* for an application (Mahmood et al. 2018), resulting in suboptimal performance in most instances.

In this paper, we challenge RL's conventional fixed time step assumption, aiming to formulate faster and more energy-efficient policies. Our approach seamlessly integrates the temporal aspect into the learning process. This modification can benefit onboard computers with limited resources so that deployed AI no longer consumes precious computing resources to compute unnecessary actions, effectively improving general system deployability. In our ap-

proach, the policy determines the following action and the duration of the next time step, making the entire learning process and applying policies *adaptive* to the specific demands of a given task. This paradigm shift follows the core principles of reactive programming (Bregu et al. 2016): as illustrated in the lower portion of Figure 1, in stark contrast to a strategy reliant on fixed execution times, adopting a dynamic execution time-based approach empowers the agent to achieve significant savings in terms of computational resources, energy consumption, and time expended. Moreover, our adaptive approach enables the integration of learning and control strategies, resulting in a unified system that enhances data efficiency and simplifies the pursuit of an optimal control strategy.

An immediate benefit of our approach is that the freed computational resources can be allocated to additional tasks, such as perception and communication, broadening the scope of RL applicability in resource-constrained robots. We view the variable control rate as promising for widely adopting RL in robotics.

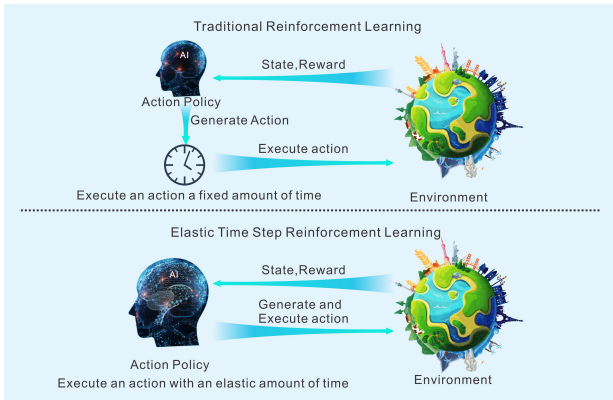


Figure 1: Comparing Elastic Time Step Reinforcement Learning and Traditional Reinforcement Learning

## Reinforcement Learning with A Fixed Control Rate

Before delving into the variable control rate RL, we provide a concise overview of fixed time step-based RL. A notable example of successful real-world reinforcement learning applications is Sony’s autonomous racing car: Sony has effectively harnessed the synergy between reinforcement learning algorithms and a foundation of dynamic model knowledge to train AI racers that surpass human capabilities, resulting in remarkably impressive performance outcomes (Wurman et al. 2022). From a theoretical perspective, Li et al. (2020) aimed to bolster the robustness of RL within non-linear systems, substantiating their advancements through simulations in a vehicular context. A shared characteristic among these studies is their dependence on a consistent control rate, typically 10 or 60 Hz. However, it is important to note that a

successful strategy does not necessarily equate to an optimal one. As previously mentioned, time is critical in determining the system’s performance, whether viewed from an application or theory perspective. The energy and time costs of completing a specific task determine an agent’s level of general efficiency. A superior control strategy should minimize the presence of invalid instructions and ensure control actions are executed only when necessary. Hence, the duration of an individual action step should not be rigidly fixed; instead, it should vary based on the dynamic demands of the task.

We have designed a variable control rate reinforcement learning method to address the time issue. This approach trains the policy to predict the time for executing the action and the action itself, adapting to dynamic changes in demand. The goal is to overcome dynamic environment uncertainty and save the agent’s computing resources. In a related study on changes in action execution time using reinforcement learning, Sharma, Srinivas, and Ravindran (2017) introduced the concept of a learning-to-repeat strategy. Essentially, they found that when an agent performs the same action with the same execution time repeatedly, it can effectively alter the action execution time. However, their approach has limitations, particularly in simulating real-world scenarios. In simulations, executing a 10-second action and executing a 1-second action ten times may appear similar. Yet, their method doesn’t account for potential changes in the agent’s physical properties in natural environments. For instance, if the mass of the agent changes while it’s performing a task, executing the same action simultaneously may not yield the same results. Moreover, the repeated execution of the same actions doesn’t optimize computing resources. Allocating these resources to other tasks, like environment awareness, could significantly benefit onboard computers with limited computing capacity.

In addition, we also noticed that Chen et al. (2021) changes the “control rate” in disguise by taking actions such as sleeping. However, it still needs a fixed control frequency to scan the agent’s status to decide whether to take sleep action as the next step. High-frequency system status scanning and calculation also cannot effectively reduce the computing load. In addition to the previously mentioned scenarios, there exists a diverse range of time-sensitive reinforcement learning tasks spanning various domains. These tasks cover multiple fields, including robotics, electricity markets, and many others (Nasiriany, Liu, and Zhu 2022; Pardo et al. 2018; Zhang, Zhang, and Qiu 2019; Yang et al. 2018). However, using a fixed control rate is a common thread among these works and systems like robots, which often lack ample computing resources, can struggle to maintain a high and fixed control rate. The algorithm we designed can solve the problem of insufficient computing resources caused by maintaining too high a frequency, and it can be applied widely. It can train almost all RL strategies based on continuous control. For example, the problem of vehicles moving in a Newtonian dynamic environment; the classic robot arm problem: one assumes that the output of the strategy set is a force set. Suppose you want to quickly grab a fragile object, such as an egg, without considering other interfer-

ences, such as the material of the robot arm. In that case, the grip strength of the robot arm and direction are essential, and the duration of the force is even more critical. Beside the robotic related application, it can also be applied on Real-Time Strategy Applications, such as AI in gaming applications (Trackmania, Genshin Impact, and etc.). Especially those application scenarios deployed on smartphones with limited computing resources.

## Reinforcement Learning with Variable Control Rate

A straightforward approach to variable time step duration is to monitor the completion of each execution action and dispatching the subsequent command. Indeed, in low-frequency control scenarios, there are typically no extensive demands for information delay or the overall time required to accomplish the task (games like Go or Chess, Silver et al. 2016, 2018). However, in applications like robotics or autonomous driving, the required control frequency can vary from very high (Hwangbo et al. 2017; Hester and Stone 2013; Hester, Quinlan, and Stone 2012) to low depending on the state of the system. Following reactive programming principles (Bregu et al. 2016), to control the system only when necessary we propose that the policy also outputs the duration of the current time step. Reducing the overall number of time steps conserves computational resources, reduces the agent’s energy consumption, and enhances data efficiency.

Unfortunately, in most RL algorithms, such as Q learning (Watkins and Dayan 1992) and the policy gradient algorithm (Sutton et al. 1999), there is no concept of the action execution time, which is considered only in few works (Ramstedt and Pal 2019; Bouteiller et al. 2021). When control frequency is taken into consideration, it is mostly related to specific control problems (Adam, Busoniu, and Babuska 2011; Almási, Moni, and Gyires-Tóth 2020), and assuming actions executed at a fixed rate.

We propose a reward policy incorporating the agent’s energy consumption and the time taken to complete a task and extend Soft Actor-Critic (Haarnoja et al. 2018a) into the Soft Elastic Actor-Critic (SEAC) algorithm, detailed in the following.

It is worth noting that for using SEAC on a robot control, an appropriate control system would be necessary for a real-world implementation, e.g. a proportional-integral-derivative controller (PID) controller (Singh, Ierapetritou, and Ramachandran 2013), an Extended Kalman filter (EKF) (Dai et al. 2019), and other essential elements. These components would need to be implemented to use SEAC into a real system environment. Nevertheless, we show that our system can indeed learn the duration of control steps and outperform established methods in a proof-of-concept implementation.

### Energy and Time Concerned Reward Policy

As shown in Figure 2, our approach tackles a multi-objective optimization challenge, in contrast to conventional single-objective reinforcement learning reward strategies. We aim

to achieve a predefined objective (metric 1) while minimizing energy consumption (metric 2) and time to complete the task (metric 3). To reduce the reward to a scalar, we introduce 3 weighting factors:  $\alpha_t$ ,  $\alpha_e$ , and  $\alpha_\tau$ , respectively assigned to our three metrics. It is important to note that we consider only the energy consumption associated with the computation of a time step (i.e. energy is linearly proportional to the number of steps) and not the energy consumption of the action itself (e.g moving a heavy object, taking a picture, etc.). Thus, our assessment of the agent’s energy usage is solely based on the *computational load*.

At the same time, it is also necessary to minimize time consumption. Reducing the number of time steps does not necessarily mean reducing the overall time consumption under variable control rates. The MDP does not constrain the time the agent takes to complete a time step. In some extreme cases, for example, the agent took *an entire year* to meet *one step* only. Although it meets with the MDP, it is unacceptable for most application scenarios. Based on the above considerations, while we pursue the number of time-step minimization, we also pursue time-consuming minimization.

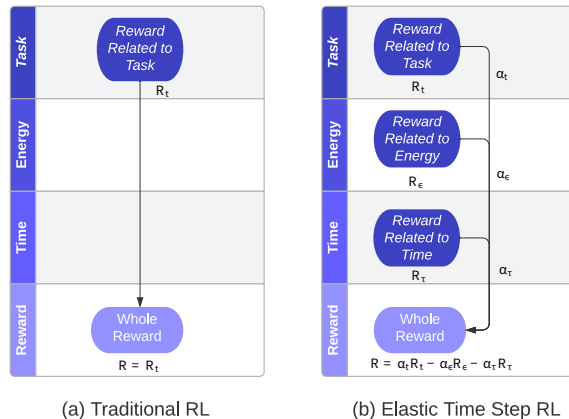


Figure 2: (a) the reward policy for traditional RL; (b) the reward policy for elastic time step RL

We assume that each action incurs a uniform energy consumption, denoted as  $\epsilon$ . The time taken to execute an action is  $\tau$ . In this context, the reward for one single step is represented by  $R$ , and the relationship can be expressed as follows:

## Reward Function

**Definition 1** The reward function is defined as:

$$R = \alpha_t \cdot R_t - \alpha_\varepsilon \cdot R_\varepsilon - \alpha_\tau \cdot R_\tau \quad (1)$$

where

$R_t = r$ ,  $r$  is the value determined by task setting;

$R_\varepsilon = \varepsilon$ ,  $\varepsilon$  is the energy cost of one time step;

$R_\tau = \tau$ ,  $\tau$  is the time taken to execute a time step.

$\alpha_t, \alpha_\varepsilon, \alpha_\tau$  are parametric weighting factors.

We determine the optimal policy  $\pi^*$ , which maximizes the reward  $R$ .

While our algorithm aims to optimize multiple objectives, we take a simplified approach using a weighted strategy. Unlike the Hierarchical Reinforcement Learning (HRL) algorithm (Dietterich 2000; Li et al. 2019), our method doesn't pursue Pareto optimality (Kacem, Hammadi, and Borne 2002; Monfared, Monabbati, and Kafshgar 2021) or involve multiple reward policies at different levels. Although our approach and HRL are designed to achieve various goals, they differ fundamentally in strategy settings. We've intentionally kept our strategy straightforward, making it user-friendly, computationally friendly, and adaptable for other algorithms. We've incorporated our reward policy into the SAC (Haarnoja et al. 2018a,b) algorithm, extending it to SEAC. Importantly, this policy isn't exclusive to SAC – it can also be applied to other RL algorithms, such as PPO (Schulman et al. 2017), TD3 (Fujimoto, Hoof, and Meger 2018), etc. This compatibility makes our algorithm easily referenceable and deployable to different applications.

### The Verification Environment Design

Our SEAC verification work requires an environment that is non-discrete time and can reflect the full impact of time on action execution. This environment is not available within existing RL environments, we establish a test environment based on Gymnasium featuring variable action execution times, shown in Figure 3:

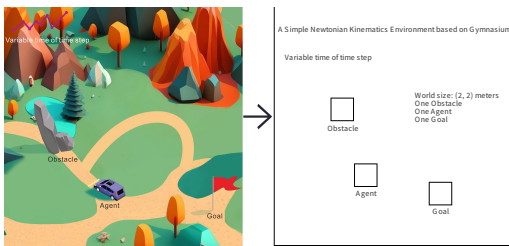


Figure 3: A simple Newtonian Kinematics environment designed for verifying SEAC based on gymnasium.

To help readers grasp our algorithm better, we will delve into the design of the verification environment and provide a detailed explanation of how we implemented the algorithm in the upcoming section. This will give a clearer picture of the practical aspects of our work.

This environment is a continuous two-dimensional (2D) and consists of a starting point, a goal, and an obstacle. The

task involves guiding an agent from the starting point to the goal while avoiding the obstacle. Upon resetting the environment, a new goal and obstacle are randomly generated. The conclusion of an episode is reached when the agent reaches the goal or encounters an obstacle. The agent is governed by Newton's laws of motion, including friction, details can be found in Definition 2 and Appendix A .

The starting point of the agent is also randomly determined. If the goal or obstacle happen to be too close to the starting point, they are reset. Similarly, if the goal is too close to the location where the obstacle was generated, the obstacle's position is reset. This process continues until all three points are situated at least 0.05 meters apart from each other on a (2 x 2) meters map. Meanwhile, the maximum force in a single step is 100.0 Newton.

There are eleven dimensions of the state in the environment: the agent's position, the position of the obstacle, the position of the goal, the speed of the agent, the duration for last time step, and the force being applied for the last time step. It is worth noting that we are indeed using historical data (i.e. the movement and duration value of the preceding step), but refrain from using recurrent neural networks (RNN) (Zaremba, Sutskever, and Vinyals 2014; Lipton, Berkowitz, and Elkan 2015). This decision stems from our concern that adopting recurrent architectures might deviate the overall reinforcement learning process from the Markov assumption (Norris 1998; Gers, Schmidhuber, and Cummins 2000): different decisions could arise from the same state due to the dynamic environment.

We consider 3 dimensions to the actions within the environment:

1. The time taken by the agent to execute the action;
2. the force being applied for the agent along the x axis;
3. the force being applied for the agent along the y axis.

For instance, an action  $a_t = (0.2, 50.0, -70.0)$  denotes that the agent is expected to apply 50.0 Newton force along the x axis and -70.0 Newton force along the y axis within 0.2 seconds. For more detailed environment settings, see Appendix A .

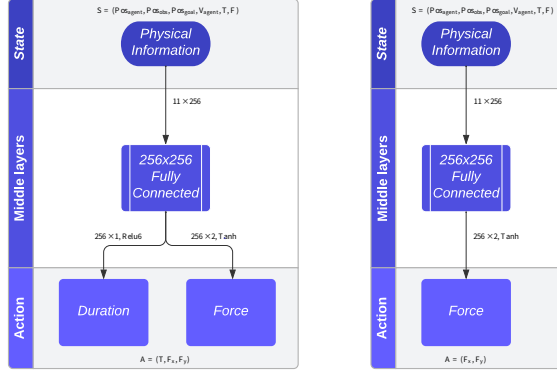
### Implementation of The SEAC

We extend the SAC algorithm to verify the validity of our Definition 1. Because we have not modified its loss functions, please refer to Haarnoja et al. (2018b) for its policy optimization.

We validate our reward strategy by taking the SAC algorithm and implementing fully connected neural networks (Müller, Reinhardt, and Strickland 1995) as both the actor and critic strategy. We assume the agent can explore the unknown environment as much as possible based on information entropy, giving a high probability that the agent can discover the optimal solution to complete the task.

As shown in Figure 4, we marked the specific values of  $S_t$  and  $A_t$  based on the environment we explained in Section 3-2 , and the network structure of the Actor Policy. This will intuitively help readers realize the difference between SEAC and SAC. In contrast to the conventional RL, in addition to the environment's state data, we take the agent's

action history values and bring them together to the form of states as the network’s input, including the time spent performing the previous action ( $T$ ), and the force in the last step ( $F_x$  and  $F_y$ ). We regard them as part of the state, because we believe position and velocity is insufficient to express the system’s inertia. This setting can ensure that the Markov process can completely describe our environment, thereby ensuring the convergence of the RL algorithm. Additionally, our approach involves an extra component at the output: the duration time  $T$  for each action.



(a) SEAC (SAC with Elastic Time Steps) (b) SAC with Fixed Time Steps

Figure 4: (a) The SEAC ActorNetwork Architecture; (b) The SAC ActorNetwork Architecture.

When the Actor Network generates the action value  $A_t$  for the next step, the controller (Figure 4) will compute a range of control-related parameters (e.g., speed, acceleration, etc.) based on the action value and time. Under the context of our test environment, The related formulas are Newton Kinematics:

#### Newton Kinematics Formulas

**Definition 2** The Newton Kinematics formulas are:

$$D_{aim} = 1/2 \cdot (V_{aim} + V_{current}) \cdot T; \quad (2)$$

$$V_{aim} = V_{current} + AT; \quad (3)$$

$$F_{aim} = mA; \quad (4)$$

$$F_{true} = F_{aim} - f_{friction}; \quad (5)$$

$$\begin{aligned} f_{friction} &= \mu mg, \text{ If } F_{aim} > f_{friction} \\ &\& V_{agent} \neq 0; \\ &= F_{aim}, \text{ If } F_{aim} \leq f_{friction} \\ &\& V_{agent} = 0. \end{aligned} \quad (6)$$

where  $D_{aim}$  is the distance generated by the policy that the agent needs to move.  $V_{agent}$  is the speed of the agent.  $T$  is the time to complete the movement generated by the policy,  $m$  is the mass of the agent,  $\mu$  is the friction coefficient, and  $g$  is the acceleration of gravity.

Through the duration and force generated by the policy, we can know the acceleration required to complete the policy and then calculate the speed. Then, we can compute the movement. However, due to friction, the actual acceleration will be inconsistent with the aimed acceleration, and the movement of the agent will be affected by Newtonian kinematics. Ultimately, the agent incorporates these actionable parameters into the environment, generating a new state and reward. This process is iterated until the completion of the task.

Our objective is for the agent to learn the optimal execution time for each step independently. We need to ensure that time is not considered as a negative value. Consequently, diverging from the single  $Tanh$  (Kalman and Kwasny 1992) output layer typical in traditional RL Actor Networks, we separate the Actor Network’s output layer into two segments: we use  $Tanh$  as the output activation for the action value, and  $ReLU6$  (Howard et al. 2017) for the output activation related to the time value.

As Definition 1, the precise reward configuration for our environment are outlined in Table 1. The hyperparameters settings can be found in Appendix B.

Table 1: Reward Policy for The Simple Newtonian Kinematics Environment

Reward Policy		
Name	Value	Annotation
r	100.0	Reach the goal
	-100.0	Crash on an obstacle
	$-1.0 \cdot D_{goal}$	$D_{goal}$ : distance to goal
$\epsilon$	1.0	Computational energy (Joule)
$\alpha_t$	1.0	Task gain factor
$\alpha_\epsilon$	1.0	Energy gain factor
$\alpha_\tau$	1.0	Time gain factor

It is noteworthy that our design does not substantially increase the model size. The recorded size of the network model in Appendix A is a mere 282.5KB after training. In comparison, the model size of the SAC network, of equivalent dimensions, is 280.5KB after training. The SEAC model is only 2KB larger, representing approximately a 7% increase in storage demand. This meticulous consideration ensures the model’s deployability.

## Experimental Results

We conducted six experiments for each of the three RL algorithms, employing various parameters within the environment described in Section III<sup>2</sup>. These experiments were conducted on a machine equipped with an Intel Core i5-13600K CPU and an NVIDIA RTX 4070 GPU, running Ubuntu 20.04. Subsequently, we selected the best-performing policy for each of these three algorithms to draw the graphs in Figures 5–8.

<sup>2</sup>Our code is publicly available at Github: <https://github.com/alpaficia/SEAC.Pytorch.release>

The frequency range for action execution spans from 1 to 100 Hz, and the agent’s force value ranges from -100 to 100 Newton. We compared our results with the original SAC (Haarnoja et al. 2018b) and PPO (Schulman et al. 2017) algorithms, both employing a fixed action execution frequency of 5.0 Hz.

We use the conventional average return graph and record the average time cost per task to clearly and intuitively represent our approach’s performance. Furthermore, we generate a chart illustrating how the variable control rate policy works in action execution frequency for four tasks with the SEAC model. Finally, we draw a raincloud graph to visualize the disparities in energy costs among these three RL algorithms for one hundred different tasks.

Appendix B provides all hyperparameter settings and implementation details. The average return results of all algorithms are shown in Figure 5, and their time-consuming results are shown in Figure 6:

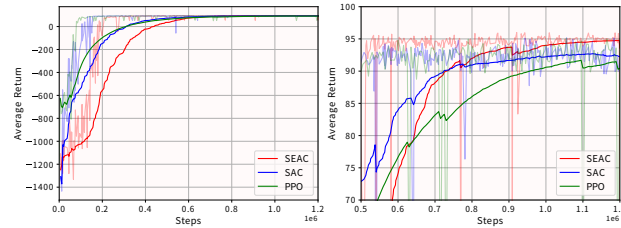


Figure 5: Average returns for three algorithms trained in 1.2 million steps. The figure on the right is a partially enlarged version of the figure on the left.

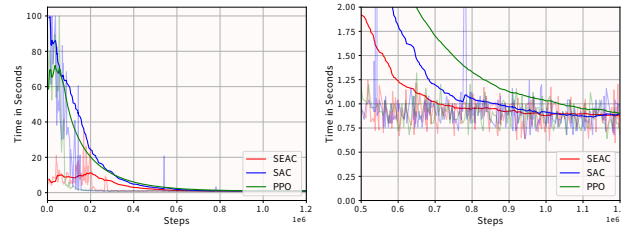


Figure 6: Average time cost per episode for three algorithms trained in 1.2 millions steps. The figure on the right is a partially enlarged version of the figure on the left.

Figure 5 and Figure 6 show that SEAC surpasses the baselines in terms of average return and time efficiency. The amount of data that SEAC needs to be trained has one more dimension than SAC and PPO (duration). So its training speed is not as fast as the above two at the beginning. However, when SEAC gradually reduces the amount of data by reducing the number of steps, its data efficiency improves significantly, starting from around 300,000 steps and finally converging before SAC and PPO around 900,000 to 1,200,000 steps. Fast training is also an exciting advantage for deployable AI. Meanwhile, SEAC, using the same pol-

icy optimization algorithm but incorporating an elastic time step, demonstrates higher and more stable final performance than SAC.

When considering the adaptation of action execution frequency within the SEAC model, we generate the variable control rate policy explanation charts for four distinct trials, as depicted in Figure 7, each utilizing different random seeds. As shown within the four charts, the first step of these SEAC policies is to use one or two *long period* steps to give the agent a large force to accelerate and to approach the goal, then use *a small time* to adjust the speed direction within a step, and then use high-frequency control rates to reach the target (subfigure 4) stably. Subfigures 3 and 4 show that it has learned to avoid obstacles.

Additionally, Figure 8 illustrates the energy cost (i.e. the number of time steps) across one hundred independent trial: as expected, SEAC minimizes energy with respect to PPO and SAC without affecting the overall average reward. It is worth noting that SAC and PPO are not optimising for energy consumption, so they are expected to have a large result spread. More interestingly, SEAC *both* reduces energy consumption *and* achieved a high reward. We maintain a uniform seed for all algorithms during this analysis to ensure fair and consistent results.

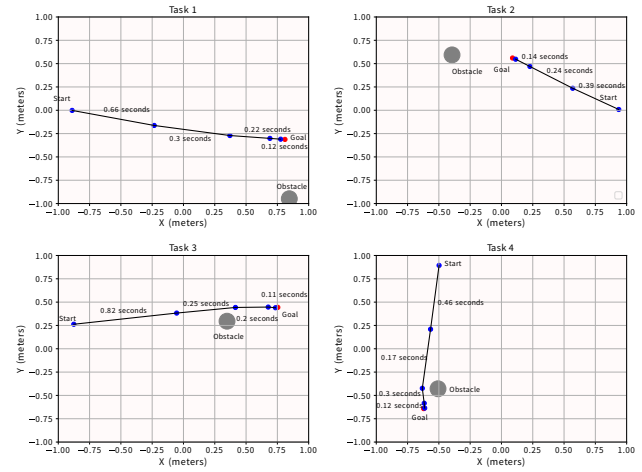


Figure 7: Four example tasks show how SEAC changes the control rate dynamically to adapt to the Newtonian mechanics environment and ultimately reasonably complete the goal.

As shown in Figure 7, the agent’s task execution strategy primarily focuses on minimizing the number of steps and the time required to complete the task. Notably, the agent often invests a substantial but justifiable amount of time in the initial movement phase, followed by smaller times for subsequent steps to arrive at the goal. This pattern aligns with our core philosophy of minimizing energy and time consumption.

Figure 8 shows that the average computing energy consumption and its standard deviation of SEAC for completing the same task are far lower than the two fixed con-

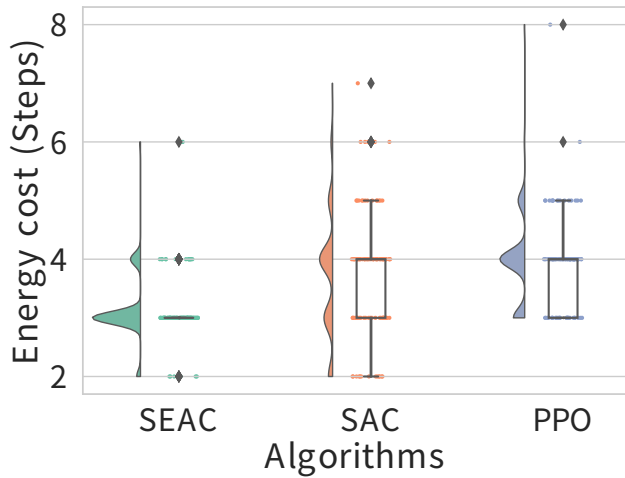


Figure 8: The energy cost for 100 trials. SEAC consistently reduces the number of time steps compared with PPO and SAC without affecting the overall average reward. Therefore, SAC and PPO are not optimizing for energy consumption and have a much larger spread.

control rate-based reinforcement learning policies as comparison objects. Compared with the SAC baseline, the average computing energy consumption is reduced by around 25% while taking less time to accomplish tasks. As we mentioned in Section IV, when the storage load increased by about 7%, the computing energy consumption dropped by around 25%, and the performance was not lost or even better. Compared with the fixed-time step RL policy, the variable-rate RL policy is undoubtedly a better choice for the deployable AI.

Furthermore, the variance in data distribution is notably reduced within the SEAC results. These findings underscore the algorithm’s heightened stability in dynamic environments, further substantiating the practicality of our variable control rate-based RL reward policy.

## Conclusions and Future Work

We propose a variable control rate-based reward policy that allows an agent to decide the duration of a time step in reinforcement learning, reducing energy consumption and increasing sample efficiency (since fewer time steps are needed to reach a goal). Reducing the number of time steps can be very beneficial when using robots with limited capabilities, as the newly freed computational resources can be used for other tasks such as perception, communication, or mapping. The overall energy reduction also increases the applicability of this policy to deployable AI on robotics.

We introduce the Soft Elastic Actor Critic (SEAC) algorithm and verify its applicability with a proof-of-concept implementation in an environment with Newtonian kinematics. The algorithm could be easily extended to real-world applications, and we invite the reader to refer to Section V and Appendix B for the implementation details.

To the best of our knowledge, SEAC is the first reinforcement learning algorithm that simultaneously outputs actions and the duration of the following time step. Although the method would benefit from testing in more realistic and dynamic settings, such as Mujoco (Todorov, Erez, and Tassa 2012) or TMRL (tmrl 2023), we believe this method presents a promising approach to enhance RL’s efficiency and energy conservation for deployment on real-world robotic systems.

## References

- Adam, S.; Busoniu, L.; and Babuska, R. 2011. Experience replay for real-time reinforcement learning control. *IEEE Transactions on Systems, Man, and Cybernetics, Part C (Applications and Reviews)*, 42(2): 201–212.
- Almási, P.; Moni, R.; and Gyires-Tóth, B. 2020. Robust reinforcement learning-based autonomous driving agent for simulation and real world. In *2020 International Joint Conference on Neural Networks (IJCNN)*, 1–8. IEEE.
- Bouteiller, Y.; Ramstedt, S.; Beltrame, G.; Pal, C.; and Binias, J. 2021. Reinforcement learning with random delays. In *International conference on learning representations*.
- Bregu, E.; Casamassima, N.; Cantoni, D.; Mottola, L.; and Whitehouse, K. 2016. Reactive control of autonomous drones. In *Proceedings of the 14th Annual International Conference on Mobile Systems, Applications, and Services*, 207–219.
- Chen, Y.; Wu, H.; Liang, Y.; and Lai, G. 2021. VarLen-MARL: A framework of variable-length time-step multi-agent reinforcement learning for cooperative charging in sensor networks. In *2021 18th Annual IEEE International Conference on Sensing, Communication, and Networking (SECON)*, 1–9. IEEE.
- Dai, Y.; Yu, S.; Yan, Y.; and Yu, X. 2019. An EKF-based fast tube MPC scheme for moving target tracking of a redundant underwater vehicle-manipulator system. *IEEE/ASME Transactions on Mechatronics*, 24(6): 2803–2814.
- Dietterich, T. G. 2000. Hierarchical reinforcement learning with the MAXQ value function decomposition. *Journal of artificial intelligence research*, 13: 227–303.
- Fujimoto, S.; Hoof, H.; and Meger, D. 2018. Addressing function approximation error in actor-critic methods. In *International conference on machine learning*, 1587–1596. PMLR.
- Gers, F. A.; Schmidhuber, J.; and Cummins, F. 2000. Learning to forget: Continual prediction with LSTM. *Neural computation*, 12(10): 2451–2471.
- Haarnoja, T.; Zhou, A.; Abbeel, P.; and Levine, S. 2018a. Soft actor-critic: Off-policy maximum entropy deep reinforcement learning with a stochastic actor. In *International conference on machine learning*, 1861–1870. PMLR.
- Haarnoja, T.; Zhou, A.; Hartikainen, K.; Tucker, G.; Ha, S.; Tan, J.; Kumar, V.; Zhu, H.; Gupta, A.; Abbeel, P.; et al. 2018b. Soft actor-critic algorithms and applications. *arXiv preprint arXiv:1812.05905*.

- Hester, T.; Quinlan, M.; and Stone, P. 2012. RTMBA: A real-time model-based reinforcement learning architecture for robot control. In *2012 IEEE International Conference on Robotics and Automation*, 85–90. IEEE.
- Hester, T.; and Stone, P. 2013. Texplore: real-time sample-efficient reinforcement learning for robots. *Machine learning*, 90: 385–429.
- Howard, A. G.; Zhu, M.; Chen, B.; Kalenichenko, D.; Wang, W.; Weyand, T.; Andreetto, M.; and Adam, H. 2017. Mobilenets: Efficient convolutional neural networks for mobile vision applications. *arXiv preprint arXiv:1704.04861*.
- Hwangbo, J.; Sa, I.; Siegwart, R.; and Hutter, M. 2017. Control of a quadrotor with reinforcement learning. *IEEE Robotics and Automation Letters*, 2(4): 2096–2103.
- Kacem, I.; Hammadi, S.; and Borne, P. 2002. Pareto-optimality approach for flexible job-shop scheduling problems: hybridization of evolutionary algorithms and fuzzy logic. *Mathematics and computers in simulation*, 60(3-5): 245–276.
- Kalman, B. L.; and Kwasny, S. C. 1992. Why tanh: choosing a sigmoidal function. In *[Proceedings 1992] IJCNN International Joint Conference on Neural Networks*, volume 4, 578–581. IEEE.
- Kingma, D. P.; and Ba, J. 2014. Adam: A method for stochastic optimization. *arXiv preprint arXiv:1412.6980*.
- Li, J.; Ding, J.; Chai, T.; Lewis, F. L.; and Jagannathan, S. 2020. Adaptive interleaved reinforcement learning: Robust stability of affine nonlinear systems with unknown uncertainty. *IEEE Transactions on Neural Networks and Learning Systems*, 33(1): 270–280.
- Li, S.; Wang, R.; Tang, M.; and Zhang, C. 2019. Hierarchical reinforcement learning with advantage-based auxiliary rewards. *Advances in Neural Information Processing Systems*, 32.
- Lipton, Z. C.; Berkowitz, J.; and Elkan, C. 2015. A critical review of recurrent neural networks for sequence learning. *arXiv preprint arXiv:1506.00019*.
- Mahmood, A. R.; Korenkevych, D.; Komer, B. J.; and Bergstra, J. 2018. Setting up a reinforcement learning task with a real-world robot. In *2018 IEEE/RSJ International Conference on Intelligent Robots and Systems (IROS)*, 4635–4640. IEEE.
- Monfared, M. S.; Monabbati, S. E.; and Kafshgar, A. R. 2021. Pareto-optimal equilibrium points in non-cooperative multi-objective optimization problems. *Expert Systems with Applications*, 178: 114995.
- Müller, B.; Reinhardt, J.; and Strickland, M. T. 1995. *Neural networks: an introduction*. Springer Science & Business Media.
- Nasiriany, S.; Liu, H.; and Zhu, Y. 2022. Augmenting reinforcement learning with behavior primitives for diverse manipulation tasks. In *2022 International Conference on Robotics and Automation (ICRA)*, 7477–7484. IEEE.
- Norris, J. R. 1998. *Markov chains. 2*. Cambridge university press.
- Pardo, F.; Tavakoli, A.; Levdiq, V.; and Kormushev, P. 2018. Time limits in reinforcement learning. In *International Conference on Machine Learning*, 4045–4054. PMLR.
- Ramstedt, S.; and Pal, C. 2019. Real-time reinforcement learning. *Advances in neural information processing systems*, 32.
- Schulman, J.; Wolski, F.; Dhariwal, P.; Radford, A.; and Klimov, O. 2017. Proximal policy optimization algorithms. *arXiv preprint arXiv:1707.06347*.
- Sharma, S.; Srinivas, A.; and Ravindran, B. 2017. Learning to repeat: Fine grained action repetition for deep reinforcement learning. *arXiv preprint arXiv:1702.06054*.
- Silver, D.; Huang, A.; Maddison, C. J.; Guez, A.; Sifre, L.; Van Den Driessche, G.; Schrittwieser, J.; Antonoglou, I.; Panneershelvam, V.; Lanctot, M.; et al. 2016. Mastering the game of Go with deep neural networks and tree search. *nature*, 529(7587): 484–489.
- Silver, D.; Hubert, T.; Schrittwieser, J.; Antonoglou, I.; Lai, M.; Guez, A.; Lanctot, M.; Sifre, L.; Kumaran, D.; Graepel, T.; et al. 2018. A general reinforcement learning algorithm that masters chess, shogi, and Go through self-play. *Science*, 362(6419): 1140–1144.
- Singh, R.; Ierapetritou, M.; and Ramachandran, R. 2013. System-wide hybrid MPC–PID control of a continuous pharmaceutical tablet manufacturing process via direct compaction. *European Journal of Pharmaceutics and Biopharmaceutics*, 85(3): 1164–1182.
- Sutton, R. S.; McAllester, D.; Singh, S.; and Mansour, Y. 1999. Policy gradient methods for reinforcement learning with function approximation. *Advances in neural information processing systems*, 12.
- tmrl. 2023. tmrl main page. <https://github.com/trackmania-rl/tmrl>.
- Todorov, E.; Erez, T.; and Tassa, Y. 2012. Mujoco: A physics engine for model-based control. In *2012 IEEE/RSJ international conference on intelligent robots and systems*, 5026–5033. IEEE.
- Watkins, C. J.; and Dayan, P. 1992. Q-learning. *Machine learning*, 8: 279–292.
- Williams, G.; Wagener, N.; Goldfain, B.; Drews, P.; Rehg, J. M.; Boots, B.; and Theodorou, E. A. 2017. Information theoretic MPC for model-based reinforcement learning. In *2017 IEEE International Conference on Robotics and Automation (ICRA)*, 1714–1721. IEEE.
- Wurman, P. R.; Barrett, S.; Kawamoto, K.; MacGlashan, J.; Subramanian, K.; Walsh, T. J.; Capobianco, R.; Devlic, A.; Eckert, F.; Fuchs, F.; et al. 2022. Outracing champion Gran Turismo drivers with deep reinforcement learning. *Nature*, 602(7896): 223–228.
- Yang, Z.; Merrick, K.; Jin, L.; and Abbass, H. A. 2018. Hierarchical deep reinforcement learning for continuous action control. *IEEE transactions on neural networks and learning systems*, 29(11): 5174–5184.
- Zanon, M.; and Gros, S. 2020. Safe reinforcement learning using robust MPC. *IEEE Transactions on Automatic Control*, 66(8): 3638–3652.



Zaremba, W.; Sutskever, I.; and Vinyals, O. 2014. Recurrent neural network regularization. *arXiv preprint arXiv:1409.2329*.

Zhang, Z.; Zhang, D.; and Qiu, R. C. 2019. Deep reinforcement learning for power system applications: An overview. *CSEE Journal of Power and Energy Systems*, 6(1): 213–225.

## Appendix:A Validation Environment Details

The Spatial Information of our environment are:

Table 2: Details of The Simple Newtonian Kinematics Gymnasium Environment

Environment details		
Name	Value	Annotation
Action dimension	3	
Range of speed	$[-2, 2]$	m/s
Action Space	$[-100.0, 100.0]$	Newton
Range of time	$[0.01, 1.0]$	second
State dimension	6	Task gain factor
World size	$(2.0, 2.0)$	in meters
Obstacle shape	Round	Radius: 5cm
Agent weight	20	in $Kg$
Gravity factor	9.80665	in $m/s^2$
Static friction coeddicient	0.6	

The state dimensions are:

State

### Definition 3 State

We have only one starting point, endpoint, and obstacle in the set environment. The positions of the endpoint and obstacle are randomized in each episode.

$$S_t = (Pos, Obs, Goal, Speed, Time, Force) \quad (7)$$

Where:

*Pos* = Position Data of The Agent in X and Y Direction,

*Obs* = Position Data of The Obstacle in X and Y Direction,

*Goal* = Position Data of The Goal in X and Y Direction,

*Speed* = Sppeed Data of The Agent for Current Step,

*Time* = The Duration data of The Agent to Execute The Last Time Step,

*Force* = Force Data of The Agent for Last Time Step in X and Y Direction.

The action dimensions are:

Action

### Definition 4 Action

Each action should have a corresponding execution duration.

$$a_t = (a_t, a_{fx}, a_{fy}) \quad (8)$$

Where:

*a<sub>t</sub>* = The time of The Agent to implement current action,

*a<sub>fx</sub>* = The Force of The Agent in X Coordinate,

*a<sub>fy</sub>* = The Force of The Agent in Y Coordinate.

## Appendix:B Hyperparameter Setting of SEAC

Table 3: Hyperparameters Setting of SEAC

Hyperparameter sheet		
Name	Value	Annotation
Total steps	3e6	
$\gamma$	0.99	Discount factor
Net shape	(256, 256)	
batch_size	256	
a_lr	2e4	Learning rate of Actor Network
c_lr	2e4	Learning rate of Critic Network
max_steps	500	Maximum steps for one episode
$\alpha$	0.12	
$\eta$	-3	Refer to SAC (Haarnoja et al. 2018b)
$T_i$	5.0	Time duration of rest compared RL algorithms, in HZ
min_frequency	1.0	Minimum control frequency, in HZ
max_frequency	100.0	Maximum control frequency, in HZ
Optimizer	Adam	Refer to Adam (Kingma and Ba 2014)
environment steps	1	
Replaybuffer size	1e6	
Number of samples before training start	$5 \cdot max\_steps$	
Number of critics	2	